

Synthetic jets on wing for aerodynamic loads redistribution

Gaetano Iuso¹, Luca Acerno¹

¹*Dipartimento di Ingegneria Aerospaziale, Politecnico di Torino, Italy*

E-mail: gaetano.iuso@polito.it, luca.acerno@polito.it

Keywords: Flow control, Synthetic jets, Virtual shaping, Load redistribution.

SUMMARY. The effects due to the forcing operated by synthetic jets on the flow evolution around a wing profile NACA 0015 have been experimentally investigated. Two independent rectangular slits along the spanwise direction generating nearly 2D synthetic jets were positioned at $x/c=0.0125$ from the leading edge. Measurements of pressure distributions on the wing, wake analysis and flow visualizations were performed for incidences $\alpha=3^\circ$ and $\alpha=6^\circ$. Variations of the forcing frequency give rise to different flow patterns especially around the leading edge in the case of forcing flow. Pressure distributions in the chordwise and spanwise direction are modified under the effects of the forcing affecting also the position of the pressure center. Virtual shaping mechanism due to the interaction between the main flow and the synthetic jets has been evidenced.

1 INTRODUCTION

Large variety of techniques for aerodynamic performances improvements have been proposed for aeronautical applications. Recently the attention is also focused on the possibility to modify aerodynamic characteristics of airfoils using fluidic devices. This approach could lead to new airplane configurations without conventional control surfaces (ailerons, flaps, spoilers, slats) achieving weight reduction, fuel consumption lessening [1]. Different approaches with the purpose to achieve airfoils lift enhancement and/or drag reduction and load redistribution have been proposed. It is proven that passive devices, like vortex generator, are effective in delaying flow separation, although they introduce drag penalty due to the parasite drag [2]. Active flow control has the advantage to vary the forcing parameters according to the flow conditions to be controlled leading to higher improvement of aerodynamic performances with respect to the passive techniques. A powerful fluidic devices aimed to modify the flow field around a wing is based on the fluidic modification of the wing shape by means of synthetic jets. Also for delay separation synthetic jets have been proved to be very efficient.

The flow field of a synthetic jet is generated by an oscillating surface under a cavity communicating with an external environment throughout a circular or a 2-D orifice. The formation and the evolution of synthetic jet are well illustrated by Smith and Glezer [3]. Glezer and Amitay [4] presented a complete review concerning the fundamentals of synthetic jets and some of their applications. Seifert et al. [5] and Duvigneau et al. [6] showed stall delay of the airfoil using synthetic jets evidencing also better efficiency [5], less power consuming and less space for air supply system[6] respect to the steady jets. Glezer [7] according to the actuation frequency of the synthetic jets highlighted two different flow control approaches. The first one is characterized by non-dimensional forcing frequency $F^+=O(1)$ which is of the same order of magnitude of the shedding frequency in the wake. This approach leads to post-stall performance enhancement by

exploiting the separating shear layer receptivity to the time periodic actuation. The second approach considers $F^+ = O(10)$ which causes synthetic jet actuation to create a small stationary flow interaction domain near the jet exit and displaces the local streamlines inducing a “virtual” change in the shape of the airfoils evidenced also by Amitay et al. [8] and Vadillo et al. [9]. The displacement of the streamlines generating virtual shaping was also demonstrated by Honoan [10] and Honoan et al. [11]. These authors studied the interaction between high frequency synthetic jets and the cross flow around a 2-D cylinder. The experiment carried out by Amitay et al. [2] concerned flow control over an “unconventional airfoil” made up by a cylindrical leading edge with a 2-D spanwise jet exit and the aerodynamic fairing based on 4-digit symmetric NACA airfoil. Generally, the actuation led to flow reattachment and recovery lift for angle of attack up to 17.5° . Also drag form reduction up to 45% was observed. Chen and Beeler [1] investigated the effects of the position of synthetic jets injection on 2-D NACA 0015 airfoils at zero angle of attack. They showed that actuation was most effective when the forcing was applied upstream the separation point. Moreover an augmentation of the lift coefficient was observed when the synthetic jet was located near the leading edge. Gillaranz et al. [12] experimentally studied the effects of synthetic jets located at 12% of chord length on NACA 0015 airfoil. At small angle of attack, from 0 to 10° , the increasing the actuation frequency caused a slight increase of lift curve slope up to 5% that scaled linearly with the frequency. At the same time the forcing caused also augmentation of $C_{l_{max}}$ up to 80%. The previous authors also observed the stall delay in the forced conditions.

Large-eddy simulation was performed by You and Moin [13] on wing profile NACA 0015 whose natural flow was forced by synthetic jets according to the experiments of Gillaranz et al. [12]. Their results confirmed the experimental evidences obtained by Gillaranz [12].

Also Duvigneau and Visonneau [6] compared results solving URANS equations with those obtained by Gillaranz et al. [12] using the same baseline flow parameters. The simulation was aimed to find the optimal forcing configuration for each angle of attack investigated using an automatic optimization algorithm. Using the optimum parameters the authors demonstrated stall delay and $C_{l_{max}}$ increasing of about 32% respect to the natural flow. Synthetic jet was used by Akçayöz et al. [14] to manipulate the flow around a NACA 0015 airfoil. The authors performed numerical simulations solving Reynolds averaged equations and conducted a parametric study through the variation of the jet exit angle γ_j , the jet exit velocity u_j and the non-dimensional forcing frequency F^+ . Their results showed that the effectiveness of flow control increased at high angles of attack. Moreover they also confirmed less effectiveness of the actuation when it was positioned after the separation point, as showed by Chen and Beeler [1].

Amitay et al. [8] carried out an experimental study on the virtual shaping effects by means of synthetic jets at low angles of attack of Clark-Y airfoil having a bump placed at $x/c = 0.22$. The actuation was placed just downstream the bump through a nearly 2-D spanwise slot. The effects induced by the forcing caused a low pressure peak near the actuation location. The peak value became more and more negative as the values of F^+ and C_μ grow. Numerical simulations performed by Vadillo et al. [9] confirmed the results obtained by Amitay et al. [4] solving RANS equation. The authors also demonstrated that drag form reduction with minimal lift penalty was achievable at low angle of attack using the “Virtual Shaping” flow control technique.

The aim of the present work is to examine the effects generated by the forcing due to synthetic jets applied for flow control over the wing profile NACA 0015. Two independent synthetic jets actuators nearly 2D, operated at frequencies up to $f = 90\text{Hz}$ in symmetric and asymmetric conditions. Low Reynolds number and low angles of attack are considered. Pressure distributions in the chordwise and spanwise direction around the airfoil were measured and shown in paper. Also wake analysis and flow visualizations were performed in both natural and forced flow.

2 EXPERIMENTAL SET UP

The experimental investigation was performed in a subsonic open circuit wind tunnel. The original test section was modified in order to mount the wing profile. The height and the width of the cross section were respectively equal to 0.9m and 0.4m while its length was equal to 1m, followed by a final portion slightly divergent whose length was equal to 2m.

In figure 1 a simplified sketch of the wind tunnel and the position of the wing model in the test section are shown.

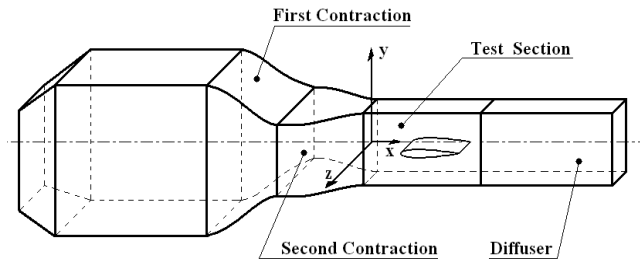


Figure 1: Sketch of the wind tunnel and the wing profile in test section

The axis coordinate system is also showed in figure 1. The origin of the cartesian system takes place in the centre of the exit of the second contraction, coincident with the entry in the test section.

The wing profile was a symmetric NACA 0015 positioned in the centre of the test section and spanning its whole width. The wing chord length was equal to 400mm and the ratio span to chord was equal to one. For a 2D experimental condition the value of this ratio is not appropriate due to the presence of corner flow that can affect the flow field around the airfoil. At moderate incidences this spurious effect was not to much influent and we concentrated our investigation in range of incidence between -3° and 9° .

The front part of the model was characterized by an hermetic spanwise chamber plenum divided in two independent and nominally equal parts, symmetrically positioned respect to the vertical plane of symmetry. The streamwise extension of the two chambers was equal to 0.125 times the wing chord length c . At the two extreme wing sections, positioned outside the test section, two pneumatic connections provided the link and the feeding between the two plenums and two independent synthetic jets actuators, one for each plenum chamber. Moreover at a streamwise distance from the leading edge equal to $0.0125c$, a rectangular slit (1mm x 200mm) for each chamber was also present. Through these nearly 2D orifices the synthetic jets were originated. The actuators consisted on the piston-cylinder oscillating system of engine airplane model. The top part of the cylinder was substituted by a cylindrical Plexiglas chamber on which top a pneumatic tube provided the connection with the spanwise plenum chambers.

The control parameter of the forcing was the oscillation frequency of the pistons. The two actuators had the possibility to operate in symmetric or asymmetric conditions in order to give rise to a symmetric or asymmetric flow control on the wing.

Static pressure taps were distributed on the upper and lower surface of the model for a total of 124 taps, along the streamwise and spanwise directions. In particular for $z/(b/2) = \pm 0.35$ two complete sets of taps were distributed along the chordwise direction on both surfaces up to $x/c=0.8$. Also along the spanwise direction for $x/c=0.0025$, $x/c=0.0375$, $x/c=0.198$ and $x/c=0.388$ pressure taps were also present.

A rake of 31 total pressure probes covering a vertical length equal to 170mm was used for the wake survey. Transverse motorized mechanism controlled by a PC provided the spanwise movements of the rake allowing the investigation of the wing profile wake.

Static and total pressure measurements were performed using two differential Scanivalve multimanometers DSA 3217 that allowed sampling of 32 input pressure through piezoresistive pressure sensors characterized by 16bit A/D converter resolution.

Measurement accuracy of the Scanivalve system was equal to 0.2% of the full scale (F.S.=±10inch H₂O). Pressure sampling was performed at 20Hz. Three and five minutes as total sampling time were considered respectively for the pressure distribution around the airfoil and for the wake measurements. The reference pressure was the static pressure of upstream undisturbed flow.

Flow visualizations were also carried out using a smoke generator emitting a smoke line. Light sheet generated by a cylindrical lens was used for illuminating vertical planes parallel the symmetry one. A digital camera provided the recording of images of the selected planes.

3 RESULTS

Preliminary investigations were performed focused on the characterization of the test section and of the synthetic jets.

3.1 Test section and synthetic jet characterizations

Total pressure distributions in three different streamwise sections : $x/c=0$, $x/c=1.65$ and $x/c = 2.5$ were performed in order to verify the flow quality in terms of uniformity distribution of the total pressure. The analysis evidenced percentage variations of total pressure distributions in the range $-0.8\% \div 1.2\%$.

The effects of the synthetic jets forcing were characterized through the values assumed by two non-dimensional parameters namely the momentum coefficient C_μ and the forcing frequency F^+ that for incompressible flow are defined respectively as :

$$C_\mu = \frac{hV_{j_{\max}}^2}{cV_\infty^2} \quad F^+ = \frac{fc}{V_\infty}$$

The two parameters are strictly connected because the synthetic jet flow field generated for each forcing frequency f in still air condition exhibits a maximum velocity $V_{j_{\max}}$ along the jet axis.

Considering a free stream velocity V_∞ , for each forcing frequency f the coefficients C_μ and F^+ are consequently linked.

The present results are related with Reynolds number equal to 250000 for which C_μ ranges from 0.0093 to 0.0390 and correspondently F^+ spans from 0.8 to 3.2.

Cross-slit velocity distribution measurements were performed on two slits for different values of the non-dimensional forcing frequency F^+ . The maximum jets velocity ranges from 3 to 4 times the free stream velocity and higher velocities were related with higher values of the non-dimensional frequency. Slightly asymmetric velocity distributions were evident between the two slits. The maximum difference of the order of 7% appears for the lower frequency. These asymmetries are probably due to the presence of pneumatic tubing differently shaped and positioned inside the two synthetic jets plenum chambers.

3.2 Validation

Chordwise pressure distributions for the natural case are first presented comparing the experimental results with those obtained using Xfoil numerical [15] code based on the boundary layer integral momentum equations. Transition was assumed free on both wing surfaces and e^n method was considered by Xfoil numerical code to evaluate the transition positions. Comparisons for $\alpha=3^\circ$ and $\alpha=6^\circ$ are respectively presented in figure 2 and figure 3. For $x/c>0.8$ the experimental data were extrapolated by linear interpolation best fit of two previous data points.

Reasonable agreement is evident for both incidences even if also some differences appear between Xfoil data and the present results, especially around the leading edge and the trailing edge. The initial part of the wing profile is characterized by the presence of plenum chambers of the synthetic jets extending up to 0.15 chord length in the streamwise direction and the two shaped covers give rise to small geometric differences and small gaps respect to the clean nominal geometry. In correspondence of the trailing edge irregular gaps can also be present due to the junction of two modules covering the upper and the lower wing surfaces. Finally 3D effects due to the low span to chord ratio also contribute to the differences. Nevertheless these pressure distributions are considered as baseline for comparisons with the forced flow.

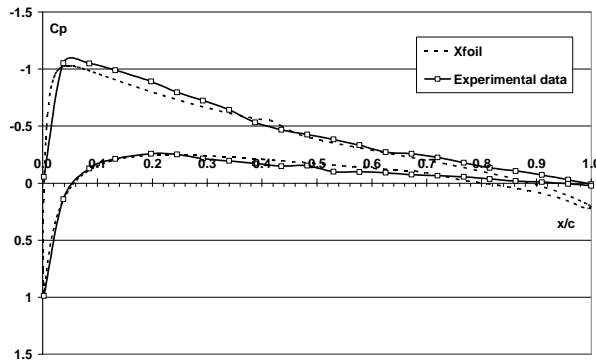


Figure 2: Pressure distributions. Comparisons between Xfoil and present results. Natural flow. $\alpha=3^\circ$

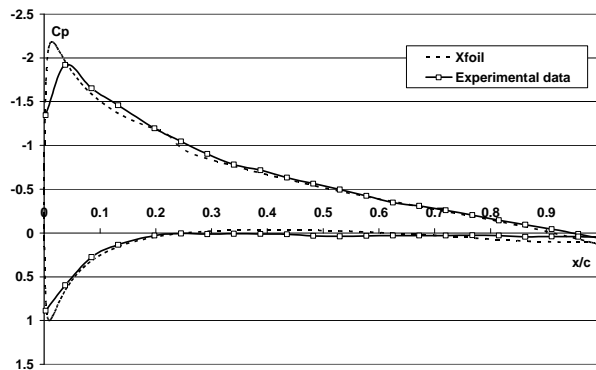


Figure 3: Pressure distributions. Comparisons between Xfoil and present results. Natural flow. $\alpha=6^\circ$.

The lift coefficients evaluated integrating the pressure distributions give rise to $C_{L_{Xfoil}}=0.323$ and $C_{L_{Exp}}=0.377$ for $\alpha=3^\circ$ and to $C_{L_{Xfoil}}=0.740$ and $C_{L_{Exp}}=0.748$ for $\alpha=6^\circ$. Better agreement is evidenced for the higher incidence.

3.3 Effects of the forcing

In figures 4 and 5 examples of chordwise and spanwise pressure distributions corresponding to asymmetric forcing conditions for $\alpha=3^\circ$ are respectively reported. Namely, in figure 4 the pressure distributions are related with the forcing operating only on the left part of the wing, $F^+=3.2$, while the right part is not forced. In the same figure also the pressure distribution corresponding to the natural flow is displayed.

As appears from the figure, the pressure distribution is significantly modified on the forced side around the slit injection positioned at $x/c=0.00125$. This modified region takes place from the leading edge and extends approximately up to $x/c=0.35$. A very intense peak of negative pressure coefficient equal to -3.14 respect to the value -1.15 of the natural case can be observed on the left forced side while on the right unforced side the pressure distribution is nearly unmodified respect to the natural. The lift coefficients on the left and right side are respectively equal to 0.414 and to 0.362 with an increment equal to 14.10% . The pitching moment, evaluated respect to the leading edge, between the forced and the unforced part remains essentially unchanged while the centre of pressure due to the increasing of the lift coefficient on the forced part, moves toward the leading edge on that part of the wing by an amount -12.45% respect to the unforced side.

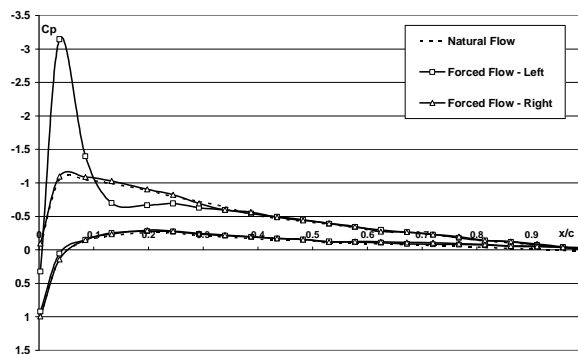


Figure 4: Chordwise pressure distributions. Natural and asymmetric forced flow. Left $F^+=3.2$ ($f=80\text{Hz}$) – Right $F^+=0$ ($f=0\text{Hz}$). $\alpha=3^\circ$.

The spanwise pressure distributions corresponding to the same forcing conditions of the previous results are displayed in figure 5 for two streamwise positions just downstream the slit injection: $x/c=0.0025$ and $x/c=0.0375$. Also the pressure distributions corresponding to the natural flow are shown. As for the streamwise pressure distributions also for the spanwise distributions the forcing deeply modify the left part of the model where the synthetic jet is activated. For both streamwise locations $x/c=0.0025$ and $x/c=0.0375$, on the right part the distributions are nearly the same of the natural flow condition. Pressure levels slightly higher respect to the natural case are evidenced for $x/c=0.25\%$ and for $z/(0.5b)*100 < -20$. For $x/c=3.75\%$ a drastic change of pressure level is present where the slit injection is activated respect to the unforced side. The value of the pressure coefficient $C_p \approx -3.5$ is maintained in average over the half wing span investigated.

Results not reported in the present paper corresponding to different forcing frequencies on the two parts of the wing confirm the evidence that just downstream the slit injection lower pressures are generated on that part of the wing where higher frequencies characterize the forcing.

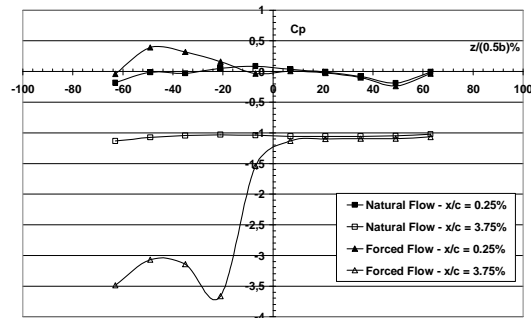


Figure 5: Spanwise pressure distributions. Natural and asymmetric forced flow. Left $F^+ = 3.2$ ($f=80\text{Hz}$) – Right $F^+ = 0$ ($f=0\text{Hz}$). $\alpha=3^\circ$.

The streamwise pressure distributions corresponding to symmetric forcing characterized by $F^+ = 2.4$ ($f=60\text{Hz}$) and $C_\mu = 0.0269$ on the two sides of the wing are displayed for incidence $\alpha=6^\circ$ in figure 6. Only the pressure distribution on the left side is shown. The effects of the forcing as for the incidence $\alpha=3^\circ$, are dominant only on the upper surface respect to the lower one. Also, the pressure distribution is to a great extent modified just downstream the injection giving rise to a peak of suction in correspondence of $x/c=0.0375$ where $C_p = -3.86$ nearly double respect to the value of the natural case.

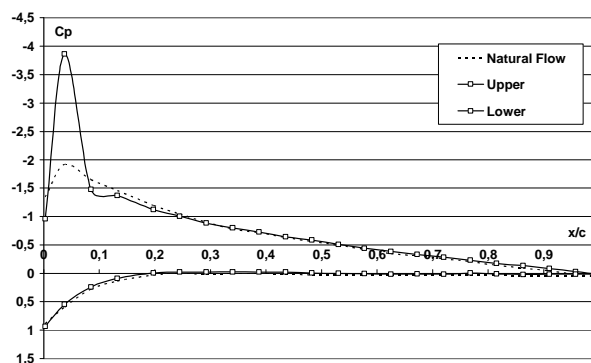


Figure 6: Chordwise pressure distributions. Natural and symmetric forced flow. Left $F^+ = 2.4$ ($f=60\text{Hz}$). $\alpha=6^\circ$

A slightly higher pressure respect to the unforced case is present for $0.085 \leq x/c \leq 0.25$. The lift and pitching moment coefficients change respectively from 0.744 and -0.203 for the natural flow, to 0.793 and -0.206 in the forced conditions. As a consequence of the pressure distribution modifications, the centre of pressure moves upstream from $x_{cp}/c=0.272$ to $x_{cp}/c=0.260$.

Results related with asymmetric forcing conditions corresponding to $F^+ = 3.2$ ($C_\mu = 0.0390$) for the left side and unforced flow on the right side are shown in figure 7.

Increasing the forcing frequency, the region of suction around the slit injection is characterized by higher negative values of pressure coefficient ($C_{p \min} = -4.68$). Also, downstream the intense suction region, the pressure recovery is once more present and extends from $x/c=0.085$ to $x/c=0.43$.

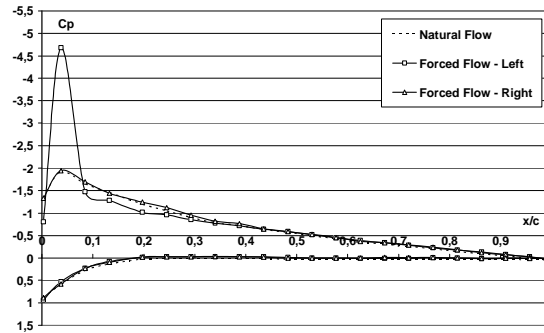


Figure 7: Chordwise pressure distributions. Natural and asymmetric forced flow. Left $F^+ = 3.2$ ($f=80\text{Hz}$), Right $F^+ = 0$. $\alpha = 6^\circ$

The right part of the wing is instead nearly unaffected by the forcing. The lift coefficients on the left and right part assume values respectively equal to 0.804 and 0.744 with an increment equal to 8%. The pitching moments remains practically unchanged and the centre of pressure moves also in this case upstream on the forced side ($x_{cp}/c = 0.251$)_{left} and remains in the same position ($x_{cp}/c = 0.273$)_{right} on the unforced part of the wing.

Results of wake survey in terms of non-dimensional velocity profiles V_w/V_∞ as a function of the normal coordinate fixed with the vertical rake extension are reported in figure 8. The forcing is characterized by nominally symmetric conditions on both slits correspondent to $F^+ = 3.2$. The mean velocity profiles are referred to different spanwise positions, namely $z=0\text{mm}$, $z=-20\text{mm}$, $z=-40\text{mm}$.

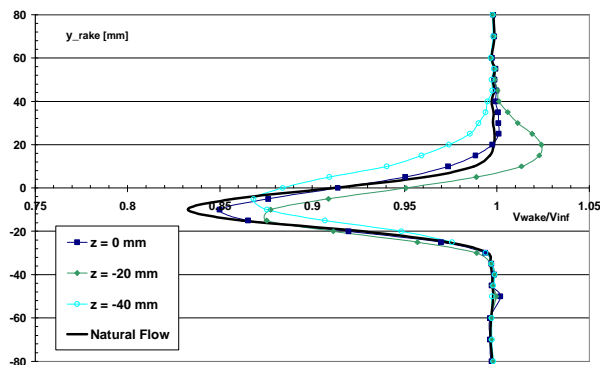


Figure 8: Wake survey. Natural and symmetric forced flow. $F^+ = 3.2$. $\alpha = 6^\circ$.

The velocity profile of the natural flow averaged over the same previous spanwise locations is also shown. The velocity distributions for the forced case show differences along the wing span, especially present for $z=-20\text{mm}$, that can be probably due to 3D effects related with the interaction synthetic jet-main stream. As for the pressure distributions along the chordwise direction also from the wake results is evident that the action of the forcing very much modify the upper part of the

wake structure respect to the lower part. The plane wake investigated in the forcing case show lower momentum deficit respect to the natural resulting in a reduced drag nearly equal to 6%.

3.4 Flow visualizations

Smoke flow visualizations for $\alpha=3^\circ$ in the case of natural and symmetric conditions ($F^+=3.2$) are shown in figure 9. Flow visualization emphasizes the presence of a bubble that takes place in the region of the injection in forcing conditions, modifying the evolution of the streamlines around the leading edge of the airfoil on the upper surface. These flow field feature is typical when the forcing is operated in the neighbourhood of the leading edge as reported also by many authors [7], [9],[10] and [11]. This synthetic jets way of employment generates the so called virtual shaping on the wing and is originated from the interaction of an appropriate synthetic jet intensity and the main stream.

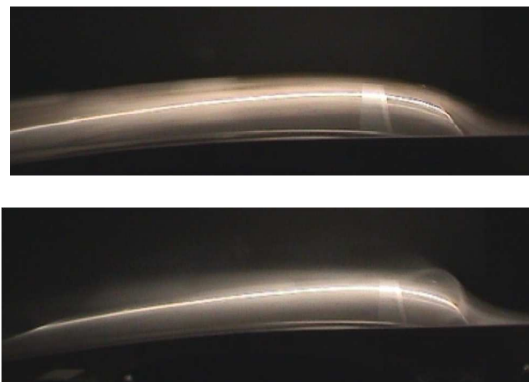


Figure 9: Upper: natural flow. Lower: forced flow $F^+=3.2$ ($C_\mu=0.0390$) $\alpha=3^\circ$.

The presence of the bubble is consistent with the pressure distributions modification on the upper surface around the leading edge in the forcing case as reported in the previous figures 4-7.

The virtual shaping change virtually the shape of the wing profile modifying the flow field around the injection similarly to the case of solid shaped body.

4 CONCLUSIONS

The effects of the forcing operated by nearly 2D independent synthetic jets emerging from two rectangular slits are reported. The flow around a wing profile NACA 0015 has been forced for incidence $\alpha=3^\circ$ and $\alpha=6^\circ$. Symmetric and asymmetric forcing were tested due to the independent actuations on two slits each of which was present on the left and right side of the wing. Results are showed for Reynolds number equal to 250000. The pressure distributions are significantly modified around the jets injection slits giving rise to intense suction around the slits injections changing the aerodynamic loads distribution in the chordwise and in the spanwise direction according to the intensity of the forcing and to the symmetric or asymmetric forcing conditions. In general increased lift coefficient and lower drag coefficient are evidenced in forced conditions for the investigated incidence. The centre of pressure moves upstream towards the leading edge and also towards the left or the right part of the wing according to the presence of the forcing on that part of the wing.

The virtual shaping mechanism has been highlighted from flow visualizations and this allows an interpretation of the pressure distributions modification in the chordwise and spanwise direction.

Acknowledgements

The present investigation is part of the project financially supported by Regione Piemonte-Bando 2004 (project E40). Thanks are due to M. Masili and M. Grivet for their collaboration during the set up phase of the experiment. The authors are also grateful to M. Orazi for the work developed during the measurements campaign of his thesis.

References

- [1] Chen, F.J., Beeler, G.B., "Virtual Shaping of a Two-dimensional NACA 0015 Airfoil Using Synthetic Jet Actuator", *AIAA paper* 2002-3273 (2002)
- [2] Amitay, M., Smith, D.R., Kibens, V., Parekh, D.E., Glezer, A., "Aerodynamic Flow Control over an Unconventional Airfoil Using Synthetic Jet Actuators", *AIAA Journal*, Vol. 39. No.3 March 2001.
- [3] Smith, B. L. and Glezer, A. "The formation and evolution of synthetic jets", *Phys. Fluids* , Vol.10, No.10, 1998, pp. 2281-2297.
- [4] Glezer A. and Amitay M. "Synthetic jets", *Annual Review of Fluid Mechanics*, Vol.34,pp. 503-529, January 2002
- [5] Seifert, A., Darabi, A., and Wygnanski, I., "Delay of Airfoil Stall by Periodic Excitation", *Journal of Aircraft*, Vol. 33, No. 4, 1996, pp. 691-69
- [6] Duvigneau, R., Visonneau, M., "Simulation and optimization of stall control for an airfoil with a synthetic jet", *Aerospace science and Technology* 10 (2006) 279-287
- [7] Glezer, A. "Fluidic-Based virtual aerosurface shaping", Paper presented at RTO AVT Specialists' Meeting on "Enhancement of NATO Military Flight Vehicle Performance by Management of Interacting Boundary Layer Transition and Separation", held in Prague, Czech Republic, 4-7 October 2004, and published in RTO-MP-AVT-111 (2004)
- [8] Amitay, M., Horvath, M., Michaux, M. and Glezer, A., "Virtual Aerodynamic Shape Modification at Low Angles of Attack using Synthetic Jet Actuators", *AIAA paper* 2001-2975 (31st AIAA Fluid Dynamics Conference & Exhibit) Anaheim, California, 11-14 June 2001
- [9] Vadillo, J.L., Agarwal, R.K., Cary, A.W., Bower, A.W., "Numerical Study of Virtual Aerodynamic Shape Modification of Airfoil Using a Synthetic Jet Actuator", *AIAA paper* 2003-4158 (33rd AIAA Fluid Dynamics Conference & Exhibit) Orlando, Florida, 11-14 June 2003
- [10] Honohan, "The interaction of Synthetic Jets with Cross Flow and the Modification of Aerodynamic Surface", *PhD dissertation*, Georgia Institute of Technology, Atlanta, GA, (2003)
- [11] Honohan, Amitay, M.,A. and Glezer, A., "Aerodynamic control using Synthetic Jets", *AIAA paper* 2000-2401, Fluids 2000 conference, Denver, CO, (2000)
- [12] Gillaranz, J.L., Traub, L. W., and Rediniotis, O.K., "Characterization of a Compact, High Power Synthetic Jet Actuator for Flow Separation Control", *AIAA paper* 2002-0127, (2002)
- [13] You, D. and Moin, P., "Large-eddy simulation of flow separation over an airfoil with synthetic jets control", *Center for Turbulence Research*, Annual Research Briefs 2006
- [14] Akçayöz, E., Erler, E., Tuncer, I.H., "Flow Control Studies over an Airfoil and an Elliptic Profile", *AIAA 2007-120*, 4th Ankara Int. Aerospace Conf. 10-12 September 2007 - METU
- [15] Dreha, M. and Youngren H. <http://web.mit.edu>